Polymer Chemistry

PAPER

View Article Online
View Journal | View Issue

Cite this: *Polym. Chem.*, 2019, **10**, 766

The emulsion polymerization induced self-assembly of a thermoresponsive polymer poly(*N*-vinylcaprolactam)†

Joonas Siirilä,[a] Satu Häkkinen[b] and Heikki Tenhu*[a]

A thermoresponsive polymer, poly(*N*-vinylcaprolactam) (PNVCL), was synthesized in an emulsion above its thermal transition temperature to produce particles *via* polymerization induced self-assembly (PISA). Two amphiphilic poly(ethylene glycol) (PEG) based xanthates were compared as macro-chain transfer agents (mCTAs) for RAFT/MADIX polymerization; thus the products were PEG-PNVCL block copolymers. Only the mCTA with a higher PEG degree of polymerization (DP) was able to stabilize the particles during the polymerization. The morphologies of the particles ranged from spherical with an inner lumen (vesicle) to spherical with a denser core and looser shell upon increasing the DP of PNVCL. This article provides proof of the polymerization induced self-assembly (PISA) of NVCL in an emulsion, producing higher morphologies (vesicles, *i.e.* spherical particles with an inner lumen) than the most commonly found spherical core–shell particles. Molecular weight analysis *via* size exclusion chromatography (SEC) revealed that the polymers had an M_n value close to the theoretical one. However, some PEG chains were not incorporated into the polymer but were observed as separated populations. This problem was resolved by reaction parameter optimization. Increasing the initiator concentration led to a decrease in polymer dispersity ($Đ$) from 1.5 to 1.2 and to all PEG being incorporated into the formed polymer. The optimized reaction parameters were used to synthesize high molecular weight PNVCL, with an M_w value of 1.27×10^6 g ml^{-1} (M_n: 810 000 g mol^{-1}), which had a PEG (5000 g mol^{-1}) end-group. The size of the high molecular weight polymer particles was in the micrometer range and thus too big for proper analysis with light scattering. The polymerization produced particles were stable at the polymerization temperature (50 °C) but disassembled upon cooling to room temperature (22 °C) due to the polymer becoming soluble. To prevent the dissolution of the polymer, the particles were stabilized through hydrogen bonding through adding salicylic acid.

Received 2nd October 2018,
Accepted 21st December 2018

DOI: 10.1039/c8py01421c

rsc.li/polymers

Introduction

PNVCL is a biocompatible polymer,[1] which exhibits LCST (lower critical solution temperature) type thermoresponsive behavior in aqueous solutions, *i.e.* the polymer turns insoluble upon heating. The phase transition temperature is close to body temperature and is dependent on the molecular mass and concentration of the polymer.[2] Thus for applications based on the amphiphilic, thermoswitchable nature of PNVCL, control over the molecular mass and a narrow molecular mass distribution are essential for optimal performance.

Studied application fields for PNVCL include its use in drug delivery,[3–11] nanoreactors for catalysis,[12,13] enzyme entrapping,[14] dye-affinity chromatography,[15] wastewater treatment,[16] flocculation[17] and thermoswitchable pressure sensitive adhesives.[18,19] A more comprehensive description of possible applications can be found in a recent review by Cortez-Lemus and Licea-Claverie.[20]

The first successful controlled polymerizations of *N*-vinylcaprolactam, NVCL, *i.e.* RAFT polymerization in bulk, were reported in 2008.[21] Following that publication, NVCL has been RAFT/MADIX polymerized by several groups, in bulk,[22,23] in various different organic solvents,[24–30] and also in water/ethanol mixtures.[31] NVCL has also been synthesized *via* ATRP[32,33] and cobalt-mediated polymerization.[34,35] All of the reported polymerizations of NVCL that have led to narrow dispersity ($Đ$ < 1.5) have, as far as we know, been conducted under conditions where PNVCL is soluble. The molecular masses have ranged from a few thousand up to 153 000 g mol^{-1}. The highest molecular mass product obtained was synthesized *via* RAFT/MADIX polymerization in solution, and

[a]*University of Helsinki, Helsinki, Finland. E-mail: heikki.tenhu@helsinki.fi*
[b]*University of Warwick, Coventry, Northern Ireland, UK*
†Electronic supplementary information (ESI) available. See DOI: 10.1039/c8py01421c

the molecular mass value corresponds to a typical upper limit for the applied method.[36]

To obtain higher molecular masses, special conditions need to be applied to suppress side reactions.[36] A good choice for water insoluble monomers is to conduct RAFT polymerization in an emulsion. In emulsion polymerization, the segregation of the polymerization loci leads to the suppression of bimolecular termination reactions, and thus allows the controlled synthesis of higher molecular mass products. Surfactant-free RAFT/MADIX emulsion polymerization has been recently reviewed by Zhou *et al.*[37] This method has been used, for example, to produce high molecular mass polystyrene[38] and poly(glycerol monomethacrylate).[39] Here, the surfactant-free RAFT/MADIX emulsion polymerization of NVCL is studied for the synthesis of high molecular mass PNVCL. Another appealing aspect of surfactant-free RAFT emulsion polymerization, and the main motivation for this work, is the formation of particles during synthesis. PNVCL based particles, which are essentially colloidal hydrogels, have been intensely studied for different biomedical applications, especially for cancer drug delivery.[4–8,11,40,41] The PNVCL particles are typically synthesized *via* free-radical emulsion/precipitation polymerization at temperatures were PNVCL is not soluble.[4–8,11,40–47] The downsides of the method include the presence of free polymer (not bound to the particles), uneven crosslinking in the particles, and the difficulty of removing surfactants from the product. We see surfactant-free emulsion polymerization as an alternative synthesis method to produce PNVCL particles. The benefits include a higher solid content, the absence of surfactants that would be left as impurities in the product, and the different expected structures of the particles because the particles are formed *via* polymerization induced self-assembly (PISA). PISA reactions in aqueous heterogeneous media have been recently reviewed in four papers.[48–51] In short, in PISA reactions, the chain extension of a solvophilic/amphiphilic chain with a solvophobic monomer leads to the self-assembly of the growing chains into well-defined particle morphologies. Ideally, the particle morphologies can be tuned through the block ratio, developing from spheres to worms to vesicles as a function of the degree of polymerization (DP) of the solvophobic block. This type of morphology transformation has commonly been observed in dispersion polymerizations where the monomer is soluble under the reaction conditions and the polymer is not. Typically in aqueous emulsion polymerization, only solid core–shell spheres are obtained.[48,49] This was true also for the, as far as we know, only reported surfactant free RAFT emulsion polymerization of NVCL.[52] In that work, NVCL was copolymerized with vinyl acetate to produce particles.

In the current report, we describe the controlled surfactant-free RAFT/MADIX emulsion polymerization of NVCL. Poly(ethylene glycol) (PEG) based xanthate is used as the chain transfer agent in the reaction. The aim was to utilize the strengths of the polymerization method, *i.e.* to synthesize high molecular mass PNVCL with control over the molecular mass and to synthesize PNVCL particles with distinct morphologies as a function of the PNVCL DP. In addition, we show that particles composed solely of PEG and PNVCL can be "frozen" *via* H-bonding, through adding salicylic acid (SA). Without SA, the assembled particles disassemble upon cooling due to PNVCL becoming soluble. This SA "freezing" is a method we have used previously as well.[9,53]

Experimental

Materials

All chemicals were used as received from suppliers unless otherwise stated. Poly(ethylene glycol) methyl ether ($mPEG_{113}$-OH; average M_n: 5000 g mol^{-1}), poly(ethylene glycol) methyl ether ($mPEG_{42}$-OH; average M_n: ~1900 g mol^{-1}), 2-bromopropionyl bromide (97%), sodium hydroxide (NaOH; ≥98%), potassium ethyl xanthogenate (96%), and Trizma base, *i.e.* 2-amino-2-(hydroxymethyl)-1,3-propanediol (Tris; ≥99.9%), were purchased from Sigma-Aldrich. *N*-Vinylcaprolactam (NVCL; 98%) was purchased from Aldrich and recrystallized twice from toluene prior to use. 2,2′-Azobis[2-(2-imidazolin-2-yl)propane]dihydrochloride (VA-044) was purchased from Wako Chemicals and recrystallized from methanol. Dichloromethane (CH_2Cl_2; 99.99%) was purchased from Fischer Scientific and dried over regenerated 4 Å molecular sieves before use. Diethyl ether (100.0%) and hydrochloric acid (HCl; 37%) were purchased from VWR Chemicals. Triethylamine (TEA; ≥99%) was purchased from Merck. Sodium hydrogen carbonate ($NaHCO_3$; 99.9%) was purchased from Fischer Scientific. Magnesium sulfate ($MgSO_4$; anhydrous; >99.5%) was purchased from Alfa Aesar. Salicylic acid (SA; 99.9%) was purchased from BDH Chemicals Ltd (Poole, England). Dimethylsulfoxide-d6 (DMSO-d6; 99.8% D) and deuterium oxide (D_2O; 99.96% D) were obtained from Euriso-Top. Dialysis was conducted using Cellu Sep T1 regenerated cellulose tubular membranes from Orange Scientific with a nominal molecular weight cut-off of 3500 Da. Purified H_2O (resistivity > 5 MΩ cm) was used throughout the study.

Synthesis of the PEG-based xanthate macro-chain transfer agents

The synthesis of two PEG-based xanthate macro-chain transfer agents (mCTA) with different PEG DP values (42 or 113) was conducted following the literature,[54] with slight modifications. The products are referred to as PEG_{42}-X and PEG_{113}-X, respectively. The synthesis scheme is presented in Fig. 1. A detailed

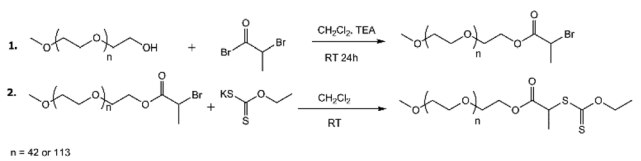

Fig. 1 The synthesis of the mCTAs, *i.e.* PEG_n-X.

synthesis description and product analysis *via* ^{1}H-NMR are presented in the ESI.†

The surfactant-free emulsion polymerization of NVCL: stabilization of the polymer particles

NVCL, VA-044, PEG$_n$-X, and buffer (0.1 M Tris; pH = 7.4) were weighed in a reaction flask. The mass of the buffer was always 10 g and the amounts of the other reagents were adjusted accordingly. The mixture was bubbled with nitrogen or argon for 1 hour at ambient temperature. The reaction mixture was then moved to a preheated oil bath: T = 50 °C. The reaction mixture was stirred with a magnetic stirrer at 400 rpm for the duration of the reaction time. Conversion samples were taken after suitable time intervals. After the conversion reached over 95% or the reaction seemed to have stopped, according to two sequential conversion measurements, the reaction flask was opened to air.

Saturated SA aqueous solution was prepared by dissolving excess SA in water for 24 hours at ambient temperature under magnetic stirring. Undissolved SA was filtered off.

Polymer particles to be analysed *via* light scattering were stabilized with SA by taking a drop from the reaction mixture with a heated pipette and diluting it at 50 °C with saturated aqueous SA solution. The polymer concentration was then approximately 0.25 mg ml^{-1}. A corresponding sample without SA was prepared by dilution with pure water. The concentrations are calculated based on weight and may deviate from the actual concentrations.

After the preparation of samples for light scattering studies, the rest of the polymerization mixture was allowed to cool to room temperature and was purified *via* dialysis and dried *via* freeze drying. The purified products were analysed with ^{1}H-NMR and SEC.

Characterization

^{1}H-NMR spectra were recorded using a 500 MHz Bruker Avance III spectrometer at 23 °C.

Size exclusion chromatography (SEC) measurements were performed with Waters ACQUITY APC apparatus connected to an ACQUITY refractive index detector. The flow rate was 0.6 ml min^{-1}. The columns used were ACQUITY APC columns of 200 Å, 450 Å and 900 Å. Measurements were performed at 30 °C. The eluent was THF. Low dispersity PMMA samples were used as a reference.

All light scattering measurements were performed using a setup involving a Brookhaven Instruments BI-200SM goniometer, a BIC-TurboCorr digital pseudo-cross-correlator, a BI-CrossCorr detector and a blue 488 nm laser (Coherent Sapphire laser 488-100 CDRH) using 10 mW of power. The sample cell was connected to a Lauda RC 6 CP thermostat.

LS measurements were performed at 50 or 22 °C. Samples were equilibrated for 30 min inside the instrument at the measuring temperature prior to measurement. Measurements were performed at 130°, 110°, 90°, 70°, 50° and 30° scattering angles.

Pseudo-cross-correlation functions of the scattered light intensity were collected at different angles using the self-beating scheme. Correlation functions were analysed using an inverse Laplace transformation (CONTIN) in the Brookhaven Instruments dynamic light scattering software. Apparent mean hydrodynamic radii from intensity weighted distributions obtained at different angles were plotted against the squared scattering vector (q^2) and the hydrodynamic radius extrapolated to zero q^2 was used as the actual hydrodynamic radius. The inverse relaxation time of the correlation function (Γ) *versus* q^2 was plotted to confirm that the movement recorded was actually translational diffusion. It was seen that the Γ *versus* q^2 dependence was linear and the fitted line went through 0.

The radius of gyration was obtained from the averaged scattering intensity simultaneously with DLS at different angles. The value was extracted from the dependence of the scattering form function on the scattering vector. From the different models tried, the Guinier model was the best for all samples studied.

SA stabilized samples were analysed with cryogenic electron microscopy (cryo-TEM). Samples were prepared with a Leica EMGP vitrification device from 3 μL aliquots on freshly glow-discharged Quantifoil R2/2 grids. The samples were observed using an FEI Talos Arctica microscope operated at 200 kV. The images were recorded at a magnification of 57 000× with an FEI Falcon 3 camera operating in linear mode.

Results and discussion

Polymerizations were performed in aqueous buffer (0.1 M TRIS) at 50 °C and a pH of 7.4. The buffer was used to prevent hydrolysis of the monomer during polymerization, which has been observed during aqueous polymerizations of NVCL.[55] All polymerizations were performed under conditions where NVCL is not soluble. The solubility of NVCL was measured to be 15 g L^{-1} in pure water at 22 °C and 35 g L^{-1} or 36 g L^{-1} in TRIS at 22 and 50 °C, respectively (experiment details presented in ESI†). The ingredients in the polymerization mixture were the buffer, initiator, monomer and a PEG-based xanthate chain transfer agent. The reaction variables, including PEG chain length, targeted PNVCL length, total concentration and initiator concentration, were systematically varied. After dialysis and drying, products were analysed in THF with size exclusion chromatography (PMMA was used as a reference) to show the dependence of the molecular mass on design and to prove that there was control of the polymerization. The particles themselves formed during the synthesis were analysed after synthesis with light scattering at 50 °C. The particles disintegrated upon cooling to ambient temperatures (Fig. 2). To study the particles *via* electron microscopy and store the particles assembled also at ambient temperatures, the particles were "frozen" *via* hydrogen bonding with salicylic acid, using a previously reported method.[9,53]

Finding a suitable DP of PEG mCTAs

A series of surfactant-free MADIX emulsion polymerizations were performed using either PEG$_{113}$-X or PEG$_{42}$-X as the

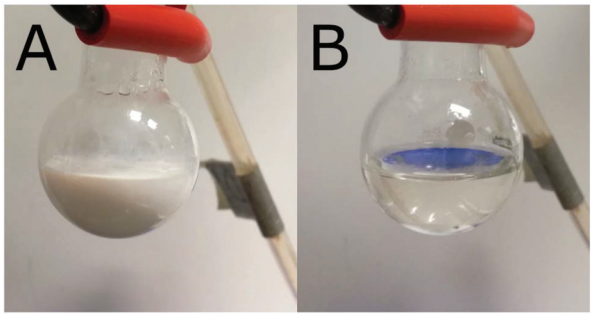

Fig. 2 Typical reaction mixtures after synthesis at (A) 50 °C and (B) 22 °C.

Table 1 Polymerizations with two different sized mCTAs

mCTA	$C(\mathrm{NVCl})_0$ (g ml^{-1})	$[M_0]:[CTA]:[I]$	Stability[a]	Conv. (%)
PEG_{42}-X	0.04	500/1/0.3	U	78
	0.08	500/1/1	U	86
	0.1	500/1/0.3	U	85
	0.1	200/1/0.3	U	83
PEG_{113}-X	0.04	500/1/0.3	S	9
	0.08	500/1/0.3	S	84
	0.1	500/1/0.3	S	97
	0.1	200/1/0.3	S	97

[a] U = unstable; S = stable. $C(\mathrm{NVCL})_0$ is the mass concentration of NVCL in the feed; [M]/[CTA]/[I] is the ratio of molar concentrations in the feed. Conv. is the conversion, determined *via* ^{1}H-NMR.

chain transfer agent in the polymerization to study the effects of the PEG DP on the synthesis. Details are presented in Table 1.

Only the polymerizations performed with PEG_{113}-X were free of coagula. In polymerizations with PEG_{42}-X at a 0.1 g ml^{-1} NVCL starting concentration, the formation of a coagulum/gel during synthesis was so extensive that the magnetic bar stopped spinning during the polymerization. Obviously, $mPEG_{42}$-X was not effective enough as a stabilizer for the polymerization. The formation of coagula was also reflected in the molecular masses of the products obtained from SEC chromatograms (Fig. 3). Polymerization with $mPEG_{42}$-X gave broad multimodal molecular masses compared to products with $mPEG_{113}$-X.

A similar but less dramatic effect was observed earlier by Rieger *at al.* when studying the impact of the PEG DP of a PEG-based trithiocarbonate macro-chain transfer agent on the emulsion copolymerization of methyl methacrylate (MMA) and *N*-butylacrylate.[56] The CTA containing the smallest example of PEG (DP ≈ 27) was too small to properly stabilize the particles, which resulted in multimodal molecular mass distribution and the formation of a small amount of aggregates. Here, the required DP of PEG is larger, probably due to better compatibility between PEG and PNVCL compared to PEG with MMA and BA. Hence, PEG is more likely to be trapped in the coalescing copolymers of PNVCL than in MMA-*co*-BA and, thus,

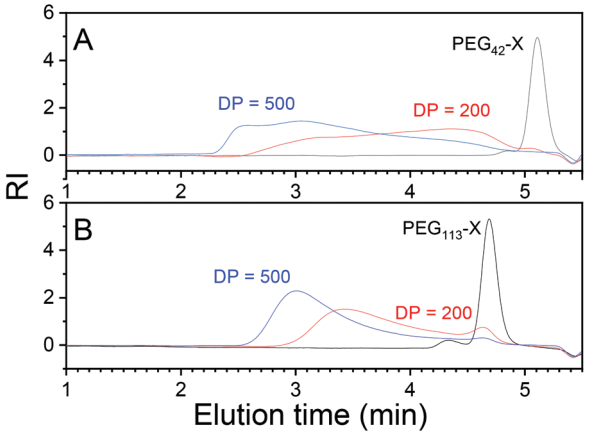

Fig. 3 SEC chromatograms of selected polymers with the use of (A) PEG_{42}-X and (B) PEG_{113}-X.

longer PEG is needed to keep the particles separated. Laukkanen *et al.* have shown that when a PNVCL-*co*-PEG_{42}-undecylmethacrylate polymer self-assembles to spherical particles in water upon heating, PEG is partly trapped inside the particles.[57] Due to the colloidal instability observed with PEG_{42}-X, PEG_{113}-X was used in the rest of the polymerizations.

The effects of reaction parameters on molar mass and control

Three series of polymerizations were performed with PEG_{113}-X as the mCTA, systematically changing the reaction parameters, *i.e.* the CTA and initiator concentrations, total concentration, and initiator concentration, one at a time. The highest monomer concentration in Table 1, 0.1 g ml^{-1}, was used as a starting point, as this concentration produced the highest conversion.

The effects of the varied parameters on the molecular mass were evaluated after dialysis and drying *via* SEC in THF. Conclusions regarding the control of polymerization were based on SEC data. In RAFT/MADIX polymerization, the molecular mass is determined *via* the ratio of monomer to chain transfer agent following eqn (1), where M_n is the number average molecular mass of the polymer, $[M]_0$ is the monomer concentration at t = 0, [CTA] is the concentration of chain transfer agent, $M_{monomer}$ is the molar mass of the monomer and M_n(CTA) is the number average molecular mass of the mCTA.

$$M_n = \frac{[M]_0}{[CTA]} \times M_{monomer} \times \text{conversion} + M_n(\text{CTA}) \quad (1)$$

The effects of mCTA (and initiator) concentration

The aim was to synthesize polymers with different PNVCL DPs. This was done by varying the mCTA to monomer ratio. The initiator concentration was adjusted accordingly to keep the ratio of mCTA to initiator constant. This approach is typical for RAFT polymerization.[36,48] In the absence of bimolecular ter-

Table 2 Polymers with different targeted PNVCL lengths

C_0(NVCL) = 0.1 g ml^{-1}, *i.e.* $[M]_0$ = 0.718 mol					
$[M_0]:[CTA]:[I]$	Conv. (%)	DP_n	Mn_{theory} (g mol^{-1})	Mn_{SEC} (g mol^{-1})	$Đ$ (M_w/M_n)
200/1/0.3	97	194	32 000	47 600	1.3
350/1/0.3	97	340	52 000	61 400	1.4
500/1/0.3	97	485	73 000	72 300	1.5
1000/1/0.3	98	980	141 000	122 000	1.3

SEC results correspond to the main peak. Conv. = conversion; DP_n = $[M]_0/[CTA]$ × Conv.; Mn_{theory} is calculated with eqn (1). Mn_{SEC} is the value obtained *via* SEC in THF using PMMA standards.

mination reactions, the amount of produced radicals should correspond to the amount of polymer chains at the end of polymerization. Thus, the ratio of initiator to mCTA determines how many of the formed polymers have an initiator derived end group and how many have an mCTA leaving group as an end group. As the leaving group of the used mCTA contains the PEG chain, the initiator to mCTA ratio determines how much of the product consists of PEG-PNVCL copolymer compared to PNVCL homopolymer. The reaction details and SEC results are presented in Table 2.

All the polymerizations proceeded to high conversions (over 95%). The molecular masses increased upon decreasing the mCTA concentration, evidencing success in synthesizing polymers with different PNVCL DPs. The M_n values obtained were relatively close to the theoretical ones calculated with eqn (1), and the dispersities ($Đ = M_w/M_n$) were all below or equal to 1.5. However, an additional peak or shoulder was observed in the molecular weight distribution (MWD) profiles presented in Fig. 4. The shoulder is only slightly shifted in comparison to mCTA and obviously corresponds to PEG_{113}-X with only a short oligomer attached. A similar shoulder was observed by Etchenausia *et al.* during the surfactant-free emulsion copolymerization of NVCL and VAc[52] and by Binauld *et al.* during the emulsion polymerization of VAc.[58] The presence of the shoulder makes the calculated DP values slightly differ from the actual DP of PNVCL. The kinetic profiles of the polymerizations, as studied *via* NMR, are presented in ESI Fig. S4.†

The effects of the total concentration

The effects of the total concentration on the molecular weight distribution were studied, as the concentration is known to influence the self-assembly process.[48] A series of polymers was synthesized where the concentration of reagents was varied while the ratio between them was kept constant. Polymerization details and SEC results are presented in Table 3. From the MWD distributions, shown in Fig. 5, it can be seen how increasing the total concentration led to a narrower MWD, with the relative size of the shoulder corresponding to small M_n compounds decreased.

The kinetics of the polymerizations were studied with NMR, and the results are presented in Fig. 6. The kinetic profiles are typical for emulsion polymerization.[59] First there is a period

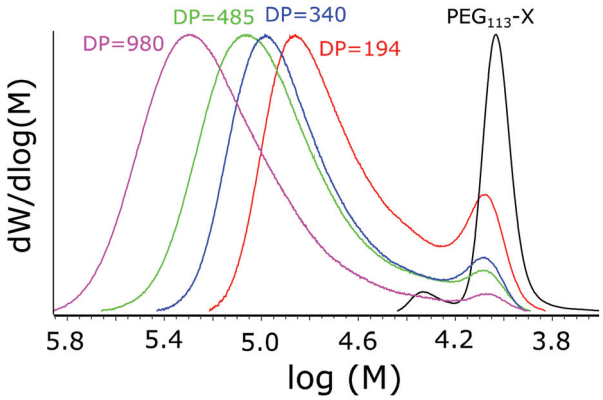

Fig. 4 MWDs of the polymers with different PNVCL DPs. PEG_{113}-X is shown for reference.

Table 3 Effects of polymerization concentration

$[M_0]/[mCTA]/[I]$ = 500/1/0.3				
$C(NVCL)_0$ (g ml^{-1})	Conv. (%)	Mn_{theory} (g mol^{-1})	Mn_{SEC} (g mol^{-1})	$Đ$ (M_n/M_w)
0.1	97	72 500	72 300	1.5
0.2	98	73 200	71 400	1.4
0.3	98	73 200	72 100	1.3

SEC results correspond to the main peak. Conv. = conversion; DP_n = $[M]_0/[I]$ × Conv.; Mn_{theory} is calculated with eqn (1). Mn_{SEC} is the value obtained *via* SEC in THF using PMMA standards.

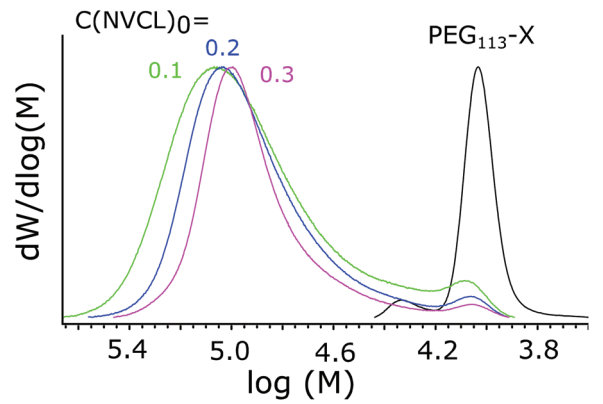

Fig. 5 MWDs of polymers synthesized with different total concentrations. The starting concentration of NVCL is marked next to each line in g ml^{-1}. PEG113-X is shown as a reference.

with an increasing rate of polymerization (interval I), secondly there is a period with a constant reaction rate, (interval II) and finally there is a period of decreasing reaction rate (interval III). Interval I is referred to as the particle nucleation period and is the period where the polymerization locus moves from the aqueous phase with a low monomer concentration to monomer-swollen particles/micelles, which have a higher monomer concentration. From Fig. 6 it can be seen how

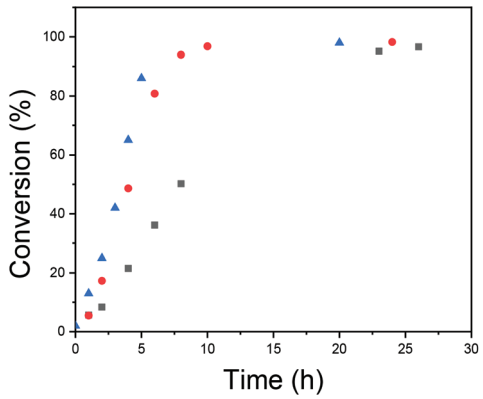

Fig. 6 Conversion *versus* time for different polymerization total concentrations: $[NVCL]_0$ = ■ 0.1 g ml^{-1}; ● 0.2 g ml^{-1}; and ▲ 0.3 g ml^{-1}.

increasing the total concentration leads to faster polymerization and, especially, to a shorter nucleation period. The rate of nucleation has also been connected to the polymer molecular weight distribution in prior literature relating to RAFT emulsion polymerizations, *i.e.* an increased nucleation rate has been shown to result in a narrower molecular weight distribution of the formed polymer.[51] The reason for this is that particles nucleated at different times will have different compositions of reagents and this introduces heterogeneity to the polymerization loci. In RAFT/MADIX polymerizations, the homogeneity of the polymerization loci is important.[60–62] The propagating chains have similar sizes due to rapid and reversible chain transfer between the chains and due to the suppression of side reactions. If the particles where the propagation takes place are different in terms of the composition of reagents and there is not sufficient exchange of material, the result will be polymers with different lengths.

A conclusion is that increasing the total concentration led to faster polymerization with a shorter nucleation period. This facilitated more mCTA being incorporated into the particles, and to more homogeneous environments for chain growth. These effects were reflected in the SEC results, as $Đ$ became smaller.

The effects of initiator concentration

As discussed above, usually in RAFT polymerizations the ratio of initiator to chain transfer agent is kept as low as possible; this still obtains the radical flux needed for polymerization but it maximizes the amount of chemically identical polymers.[36,48] However, Yan *et al.* have described a broadened MWD when decreasing the initiator concentration in the seeded RAFT emulsion polymerization of styrene.[60] The effect was explained *via* differences between active and inactive particles due to an insufficient flux of radicals that produce heterogeneous conditions for chain growth in different particles. Increasing the initiator concentration is also expected to increase the rate of reaction and shorten the nucleation period, which has already been connected to better M_n control in an above section. For these reasons, the effects of initiator concentration were studied.

Table 4 The synthesis of polymers with different initiator concentrations

C_0(NVCL) = 0.1 g ml^{-1} *i.e.* $[M]_0$ = 0.718 mol/l				
$[M_0]:[CTA]:[I]$	Conv. (%)	Mn_{theory} (g mol^{-1})	Mn_{SEC} (g mol^{-1})	$Đ$ (M_n/M_w)
500/1/0.3	97	72 500	72 300	1.5
500/1/0.6	99	73 900	74 700	1.2
500/1/0.9	100	74 600	75 700	1.2

SEC results correspond to the main peak. Conv. = conversion; DP_n = $[M]_0/[I]$ × Conv.; Mn_{theory} is calculated with eqn (1). Mn_{SEC} is the value obtained *via* SEC in THF using PMMA standards.

The reaction details and SEC data are presented in Table 4. From the MWDs presented in Fig. 7, it can be seen how increasing the initiator concentration reduces the width of the distribution and how the fraction containing smaller polymers disappears. Kinetic data is presented in Fig. 8. From the data, it can be seen how increasing the initiator concentration led to

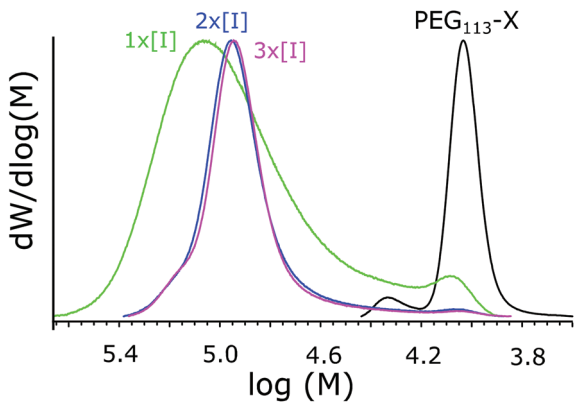

Fig. 7 MWDs of polymers synthesized with different initiator concentrations.

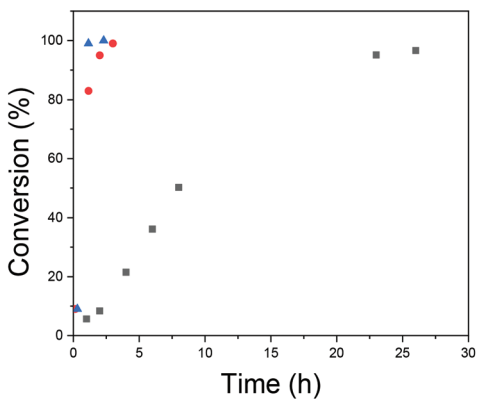

Fig. 8 Conversion *versus* time with different initiator concentrations: ■ [I]; ● 2 × [I]; ▲ 3 × [I].

faster polymerization, as was expected. The effect of increasing the initiator concentration on the MWDs and the kinetics was stronger compared to that of increasing the total concentration. Thus, we see increasing the initiator concentration as being the preferred way to improve control over polymerization. However, it has to be noted that a narrow MWD does not guarantee chemically homogenous polymers and the ratio between the homopolymers and copolymers produced needs to be studied.

The synthesis of high molecular mass PNVCL

Surfactant-free RAFT emulsion polymerization is known to be well-suited to the synthesis of high molecular mass polymers.[36–39] Observations from previous polymerizations were used to design the synthesis of a high molecular weight polymer. The selected monomer/PEG_{113}-X/initiator ratio was 6000/1/0.9 and the initial NVCL concentration was 0.1 g ml^{-1}. A stable, coagulum-free dispersion was obtained in 20 h with 98% monomer conversion.

According to SEC data, the M_n value of the polymer was 350 000 g mol^{-1} and $Đ$ was 1.5 (the chromatogram is presented in the ESI, Fig. S6†). This is, however, believed to be an underestimate caused by a few factors. The first of these is the difference between the MMA standard and the studied copolymers. Finding SEC standards for a series of copolymers (PNVCL-PEG) where the size of the other block increases from a few tens of thousands to close to million is obviously a challenge and might be impossible. The second issue is that the well-known problem of polymer adsorption to the stationary phase gets more severe upon increasing the molar mass. Hence, the results for the high molecular weight polymer from SEC can be used only to describe the relatively narrow molecular weight distribution. For the actual molecular weight analysis, we rely on static light scattering, which gives an absolute M_w value. The M_w according to light scattering analysis is 1.27 million g mol^{-1} and the analysis details are presented in the ESI.† The M_n value of 847 000 g mol^{-1} is obtained by calculating M_n from the light scattering M_w value and using the $Đ$ value of 1.5 from SEC. The theoretical M_n value is 823 000 g mol^{-1}. From ^{1}H-NMR end-group analysis, we obtain an M_n value of 810 000 g mol^{-1} (the ^{1}H-NMR spectra and calculations are presented in the ESI†).

Based on experimental evidence, we conclude the polymer to have an M_n value of 810 000 g mol^{-1} and a M_w value of 1270 000 g mol^{-1} ($Đ$ = 1.56). According to our knowledge, this is the highest molecular mass value achieved for PNVCL synthesized in a controlled manner, *i.e.* having such a low $Đ$ value. The achievement is impressive considering the high monomer conversion (98%) and over 90% yield after purification.

Particle sizes and shapes

As the main motivation behind this work, particle shape and morphology were studied. In the PISA concept, the morphology of the self-assembled particles is dictated by the block ratio. Because of this, we focus on the polymers described in Table 2. First, particles formed through self-assembly during polymerization were investigated *via* light scattering at 50 °C. The samples taken from the reaction mixtures were not allowed to cool before measurement. Light scattering data is given in Table 5.

Table 5 Light scattering data for particles with different PNVCL lengths

$[M_0]:[CTA]:[I]$	DP of PNVCL	D_h [a] (nm)	R_g/R_h [a]	D_h [b] (nm)	R_g/R_h [b]
200/1/0.3	194	190	0.85	220	1.07
350/1/0.3	340	180	0.80	210	0.82
500/1/0.3	485	225	0.76	220	0.7
1000/1/0.3	980	275	0.73	290	0.65

[a] Measured at 50 °C from a H_2O sample [b] Measured at 22 °C from salicylic acid "frozen" particles.

Hydrodynamic radius (R_h) values are presented in Table 5 in the form of hydrodynamic diameter ($D_h = 2 \times R_h$) to be consistent with the literature on PNVCL-based microgel particles.[4–8,11,41–43,47] The hydrodynamic radii of the particles stayed relatively constant upon decreasing the mCTA concentration, with the polymer with the highest PNVCL DP differing from the others by being clearly larger. R_h was expected to increase upon decreasing the mCTA concentration, as the mCTA acts as a dispersion stabilizer and decreasing the stabilizer content usually results in increased particle size.

Radius of gyration (R_g) values were obtained from the angular dependence of the normalized averaged scattering intensity measured at several angles. The ratio of the two radii, R_g/R_h, is known to reflect the shape and mass distribution of scattering objects.[63–67] 0.775 is the theoretical value for a compact sphere, where mass is distributed homogenously through the particle.[66] Hydrogel particles with a dense core and looser, freely dangling chains in the shell show typical R_g/R_h values of around 0.6.[64,67] For vesicles and polymersomes where all the mass is located on the surface of the particle, the R_g/R_h value should theoretically be 1.[63] R_g/R_h = 0.944 has been reported for lecithin vesicles.[65] An R_g/R_h value of 0.86 corresponds to a vesicle where the wall thickness equals the diameter of the inner lumen.[68] Values of above 1 are no longer strictly spherical objects. 1.5 is a typical R_g/R_h value for a random coil.[66]

R_g/R_h values for the synthesized particles are given in Table 5. The value decreases as the DP of PNVCL increases. This indicates that in particles of PNVCL with a higher DP, the mass is located closer to the core.

Laukkanen *et al.* stabilized thermal self-assemblies of PNVCL-*co*-PEG-alkylmethacrylate polymers with phenols to preserve their integrity at ambient temperatures.[9,53] The stabilization was based on hydrogen bonding and the stabilized particles were referred to as "frozen", as they were no longer thermoresponsive. Here, salicylic acid was used to stabilize the assembled particles at 50 °C and pH 2.6. The particles were stable after cooling and were studied *via* LS. The R_h and R_g values at 22 °C are presented in Table 5. The "frozen" particles

are slightly larger at 22 °C than at 50 °C. Upon cooling, the mass distribution changes slightly, highlighting the differences between particles with different PNVCL DPs.

The "frozen" particles, whose data is presented in Table 5, were imaged with cryogenic transmission electron microscopy. Images are presented in Fig. 9. The same particle size trend with decreasing [mCTA] was observed with cryo-TEM and LS. The particles with the lowest PNVCL DP had a lighter "eye" in the center of the particles. This agrees with the LS data, which shows larger R_g/R_h values for these particles. As the DP of PNVCL is increased from 194 to 485, the particles turn more homogenous, with only slight changes in size according to both LS and cryo-TEM. The particles with a PNVCL DP of 980 differ by being larger and having a denser core.

These observations correspond to the morphological transformation of vesicles where the membrane grows solely inwards as a function of the solvophobic block length, leading the lumen/inner encapsulated fluid phase to become smaller and finally non-existent. This behaviour has been previously observed by Armes *et al.* for the dispersion PISA polymerization of poly(2-hydroxypropyl methacrylate) using a poly(glycerol monomethacrylate) mCTA, and was suggested to be universal.[69] For the polymerization series in Table 5, the lumen gets smaller as the PNVCL DP is increased from 194 to 485. The polymer with a DP of 485 does not actually have a lumen. Further increasing the PNVCL DP to 980 resulted in larger particles, as there was no lumen where the membrane could grow: the particle had grown outwards.

Our current results show that self-assembly takes place during polymerization and results in particles with distinctly different morphologies. To create worms or vesicles containing larger lumens, we suggest aiming to lower the PNVCL DP.

The cryo-TEM images also shed light on the surprisingly high R_g/R_h ratio for the "frozen" particles with the shortest PNVCL length (DP = 194). In the images, some big multicore particles were observed (Fig. 10), which presumably were formed when the "frozen" particle solution was cooled from 50 °C to 22 °C and PNVCL became more solvophilic. The increased solvophilicity facilitated the fusion of the particles. It seems that for lower PNVCL lengths (DP ≤ 194), the interactions with SA are not enough to allow particles to keep their shape upon cooling.

Particle size and shape analysis was performed with LS also for other polymerization series, *i.e.* for polymerizations with varying initiator concentrations and polymerizations with different total concentrations. The effects of these parameters on particle shape were marginal. The results are presented in ESI Tables S1 and S2.†

Detailed LS analysis was not performed on the large M_n PNVCL due to its large size and seemingly broad particle size distribution (bimodal particle size). cryo-TEM images of the largest polymer are presented in the ESI† and show the presence of 1.3 μm spherical particles. In addition, a small amount (3/12) of smaller, approximately 400 nm particles was observed.

The dilution of SA "frozen" particles

A dilution experiment was carried out with one of the SA "frozen" particles. Upon dilution with pure water, the scattering intensity decreased in a linear fashion with concentration, but the size of the particles remained unchanged until a criti-

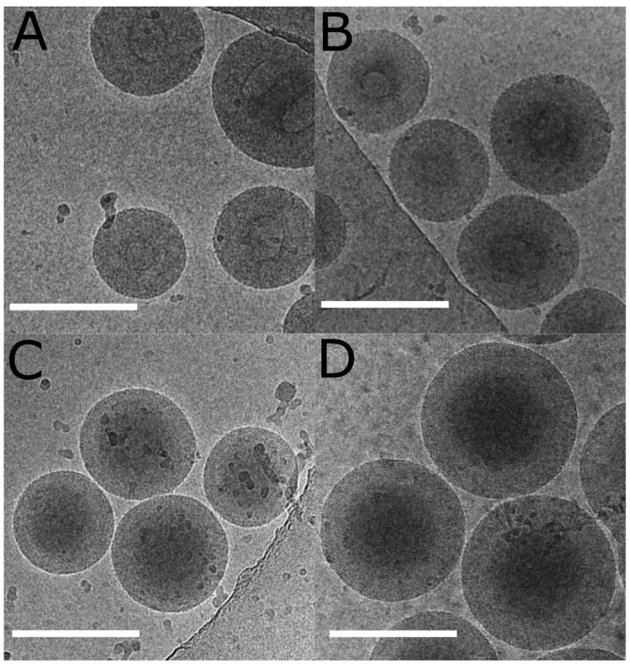

Fig. 9 Cryo-TEM images of the SA "frozen" dispersions whose data is presented in Table 5: (A) DP = 194; (B) DP = 340; (C) DP = 485; and (D) DP = 980. The scale bar is 200 nm.

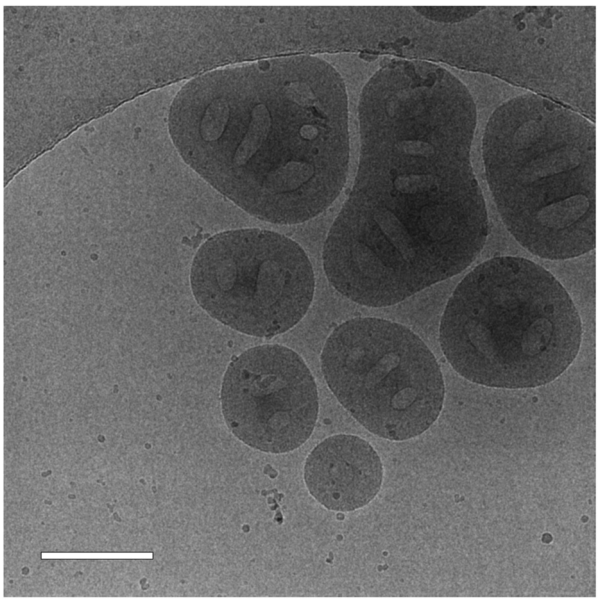

Fig. 10 A cryo-TEM image of a SA "frozen" dispersion with a PNVCL DP of 194. The scale bar is 200 nm.

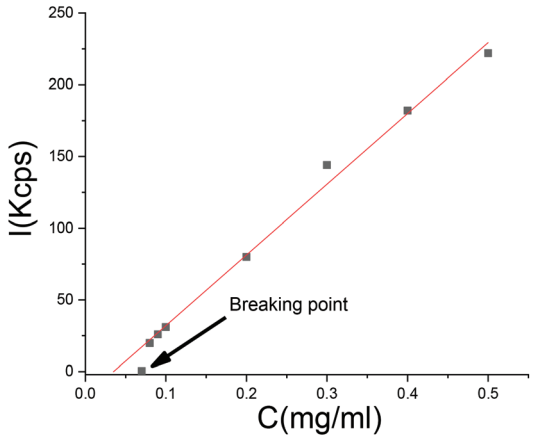

Fig. 11 A dilution test on SA crosslinked particles.

cal point where the linear dependency of the scattering intensity on concentration was lost. At this point, which we refer to as the breaking point, the intensity diminished to a value close to the scattering of pure water (Fig. 11). Before the breaking point, the particle size was independent of dilution. At the breaking point, the scattering intensity decreased to a level too low for particle size analysis. We conclude that there exists an equilibrium between SA in the aqueous phase and in the particles, respectively. At a certain dilution, the particles do not contain enough salicylic acid anymore and the polymer dissolves.

Conclusions

Successful RAFT/MADIX emulsion polymerizations of NVCL were performed in aqueous buffer at 50 °C using a PEG based macro-chain transfer agent. Molecular masses increased according to design. PEG-PNVCL block copolymers were obtained with M_n values close to the targeted M_n values, from 32 000 to 810 000 g mol^{-1}, with moderate dispersities ($Đ \leq 1.6$) and high conversions (over 95%). The crude products of the polymerizations were dispersions formed *via* PISA. This is the first time pure NVCL has been shown to undergo a PISA reaction. The particle shape was dictated by the DP of PNVCL. Particles with a PNVCL DP of 194 or 380 were vesicle type, with an inner lumen. Particles with a higher PNVCL DP (485 or 980) had denser cores and looser shells. The self-assembled spherical particles disintegrate upon cooling, due to the polymer becoming soluble. The particles remain self-assembled upon cooling if stabilized *via* hydrogen bonding with salicylic acid. From studies on the effects of initiator concentration and total concentration, it can be concluded that $Đ$ and the reaction time can be decreased by increasing either of these parameters. Increasing the initiator concentration had the strongest effect. The reaction time could be reduced from 20 h to 2 h and $Đ$ could be decreased from 1.5 to 1.2 upon tripling the initiator concentration when synthesizing PNVCL with a targeted DP of 500.

Conflicts of interest

There are no conflicts to declare.

Acknowledgements

The cryoEM unit and HiLIFE, University of Helsinki are acknowledged for the cryo-EM data collection. Vladimir Aseyev is acknowledged for valuable discussion concerning the light scattering results. The Academy of Finland is acknowledged for financial support (project number 307475).

References

1 H. Vihola, A. Laukkanen, L. Valtola, H. Tenhu and J. Hirvonen, *Biomaterials*, 2005, **16**, 3055–3064.
2 F. Meeussen, E. Nies, H. Berghmans, S. Verbrugghe, E. Goethals and F. Du Prez, *Polymer*, 2000, **41**, 8597–8602.
3 P. Mani, J. J. Grailer, D. A. Steeber and G. Shaoqin, *Macromol. Biosci.*, 2009, **9**, 744–753.
4 K. Madhusudana Rao, B. Mallikarjuna, K. S. V. Krishna Rao, S. Siraj, K. Chowdoji Rao and M. C. S. Subha, *Colloids Surf., B*, 2013, **102**, 891–897.
5 Y. Wang, J. Nie, B. Chang, Y. Sun and W. Yang, *Biomacromolecules*, 2013, **14**, 3034–3046.
6 K. Sudhakar, K. Madhusudana Rao, M. C. S. Subha, K. Chowdoji Rao and E. Rotimi Sadiku, *Polym. Sci., Ser. B*, 2015, **57**, 638–644.
7 N. Sanoj Rejinold, M. Muthunarayanan, V. V. Divyarani, P. R. Sreerekha, K. P. Chennazhi, S. V. Nair, H. Tamura and R. Jayakumar, *J. Colloid Interface Sci.*, 2011, **360**, 39–51.
8 M. A. González-Ayón, J. A. Sañudo-Barajas, L. A. Picos-Corrales and A. Licea-Claverie, *J. Polym. Sci., Part A: Polym. Chem.*, 2015, **53**, 2662–2672.
9 V. Henna, L. Antti, T. Heikki and H. Jouni, *J. Pharm. Sci.*, 2008, **97**, 4783–4793.
10 H. Vihola, A. Laukkanen, J. Hirvonen and H. Tenhu, *Eur. J. Pharm. Sci.*, 2002, **16**, 69–74.
11 S. Lou, S. Gao, W. Wang, M. Zhang, Q. Zhang, C. Wang, C. Li and D. Kong, *J. Appl. Polym. Sci.*, 2014, **131**, 41146.
12 H. Jia, D. Schmitz, A. Ott, A. Pich and Y. Lu, *J. Mater. Chem. A*, 2015, **3**, 6187–6195.
13 X. Li, T. Cai and E. Kang, *Macromolecules*, 2016, **49**, 5649–5659.
14 I. Y. Galaev and B. Mattiasson, *Biotechnol. Tech.*, 1992, **6**, 353–358.
15 I. Y. Galaev, C. Warrol and B. Mattiasson, *J. Chromatogr. A*, 1994, **684**, 37–43.
16 E. Churilina, P. Sukhanov, Y. Korenman and G. Shatalov, *Russ. J. Appl. Chem.*, 2010, **83**, 1054–1058.
17 G. V. Shatalov, V. N. Verezhnikov, E. V. Churilina, V. A. Kuznetsov and T. N. Poyarkova, *Russ. J. Appl. Chem.*, 2003, **76**, 1839–1843.

18 K. A. Bovaldinova, M. M. Feldstein, N. E. Sherstneva, A. P. Moscalets and A. R. Khokhlov, *Polymer*, 2017, 10–20.
19 M. M. Feldstein, K. A. Bovaldinova, E. V. Bermesheva, A. P. Moscalets, E. E. Dormidontova, V. Y. Grinberg and A. R. Khokhlov, *Macromolecules*, 2014, **47**, 5759–5767.
20 N. A. Cortez-Lemus and A. Licea-Claverie, *Prog. Polym. Sci.*, 2016, **53**, 1–51.
21 D. Wan, Q. Zhou, H. Pu and G. Yang, *J. Polym. Sci., Part A: Polym. Chem.*, 2008, **46**, 3756–3765.
22 L. Etchenausia, A. M. Rodrigues, S. Harrisson, E. Deniau Lejeune and M. Save, *Macromolecules*, 2016, **49**, 6799–6809.
23 L. Shao, M. Hu, L. Chen, L. Xu and Y. Bi, *React. Funct. Polym.*, 2012, **72**, 407–413.
24 V. Kozlovskaya, F. Liu, B. Xue, F. Ahmad, A. Alford, M. Saeed and E. Kharlampieva, *Biomacromolecules*, 2017, **18**, 2552–2563.
25 J. Liu, C. Detrembleur, M. De Pauw-Gillet, S. Mornet, E. Duguet and C. Jerome, *Polym. Chem.*, 2014, **5**, 799–813.
26 F. Jia, S. Wang, X. Zhang, C. Xiao, Y. Tao and X. Wang, *Polym. Chem.*, 2016, **7**, 7101–7107.
27 N. A. Cortez-Lemus and A. Licea-Claverie, *Polymers*, 2018, **10**, 20.
28 X. Zhao, O. Coutelier, H. H. Nguyen, C. Delmas, M. Destarac and J. Marty, *Polym. Chem.*, 2015, **6**, 5233–5243.
29 M. Karesoja, E. Karjalainen, S. Hietala and H. Tenhu, *J. Phys. Chem. B*, 2014, **118**, 10776–10784.
30 M. Beija, J. Marty and M. Destarac, *Chem. Commun.*, 2011, **47**, 2826–2828.
31 I. Van Nieuwenhove, S. Maji, M. Dash, S. Van Vlierberghe, R. Hoogenboom and P. Dubruel, *Polym. Chem.*, 2017, **8**, 2433–2437.
32 S. Pooja, S. Ambika and K. Rajesh, *J. Polym. Sci., Part A: Polym. Chem.*, 2012, **50**, 1503–1514.
33 X. Jiang, Y. Li, G. Lu and X. Huang, *Polym. Chem.*, 2013, **4**, 1402–1411.
34 M. Hurtgen, J. Liu, A. Debuigne, C. Jerome and C. Detrembleur, *J. Polym. Sci., Part A: Polym. Chem.*, 2012, **50**, 400–408.
35 A. Kermagoret, C. Fustin, M. Bourguignon, C. Detrembleur, C. Jérôme and A. Debuigne, *Polym. Chem.*, 2013, **4**, 2575.
36 S. Perrier, *Macromolecules*, 2017, **50**, 7433–7447.
37 J. Zhou, H. Yao and J. Ma, *Polym. Chem.*, 2018, **9**, 2532–2561.
38 X. Zhang, D. Liu, X. Lv, M. Sun, X. Sun and W. Wan, *Macromol. Rapid Commun.*, 2016, **37**, 1735–1741.
39 C. P. Jesson, V. J. Cunningham, M. J. Smallridge and S. P. Armes, *Macromolecules*, 2018, **51**, 3221–3232.
40 S. Bian, J. Zheng, X. Tang, D. Yi, Y. Wang and W. Yang, *Chem. Mater.*, 2015, **27**, 1262–1268.
41 N. S. Rejinold, R. G. Thomas, M. Muthiah, K. P. Chennazhi, I. Park, Y. Y. Jeong, K. Manzoor and R. Jayakumar, *RSC Adv.*, 2014, **4**, 39408–39427.
42 M. A. Gonzalez-Ayon, N. A. Cortez-Lemus, A. Zizumbo-Lopez and A. Licea-Claverie, *Soft Mater.*, 2014, **12**, 315–325.
43 A. Imaz and J. Forcada, *J. Polym. Sci., Part A: Polym. Chem.*, 2008, **46**, 2766–2775.
44 A. Laukkanen, S. K. Wiedmer, S. Varjo, M. Riekkola and H. Tenhu, *Colloid Polym. Sci.*, 2002, **280**, 65–70.
45 A. Laukkanen, S. Hietala, S. L. Maunu and H. Tenhu, *Macromolecules*, 2000, **33**, 8703–8708.
46 F. Schneider, A. Balaceanu, A. Feoktystov, V. Pipich, Y. Wu, J. Allgaier, W. Pyckhout-Hintzen, A. Pich and G. J. Schneider, *Langmuir*, 2014, **30**, 15317–15326.
47 A. Imaz and J. Forcada, *J. Polym. Sci., Part A: Polym. Chem.*, 2008, **46**, 2510–2524.
48 S. L. Canning, G. N. Smith and S. P. Armes, *Macromolecules*, 2016, **49**, 1985–2001.
49 S. Chen, P. Shi and W. Zhang, *Chin. J. Polym. Sci.*, 2017, **35**, 455–479.
50 B. Charleux, G. Delaittre, J. Rieger and F. D'Agosto, *Macromolecules*, 2012, **45**, 6753–6765.
51 M. J. Monteiro and M. F. Cunningham, *Macromolecules*, 2012, **45**, 4939–4957.
52 L. Etchenausia, A. Khoukh, E. Deniau Lejeune and M. Save, *Polym. Chem.*, 2017, **8**, 2244–2256.
53 A. Laukkanen, L. Valtola, F. M. Winnik and H. Tenhu, *Polymer*, 2005, **18**, 7055–7065.
54 J. Liu, C. Detrembleur, M. De Pauw-Gillet, S. Mornet, E. Duguet and C. Jérôme, *Polym. Chem.*, 2014, **5**, 799–813.
55 A. Imaz, J. I. Miranda, J. Ramos and J. Forcada, *Eur. Polym. J.*, 2008, **44**, 4002–4011.
56 J. Rieger, G. Osterwinter, C. Bui, F. Stoffelbach and B. Charleux, *Macromolecules*, 2009, **42**, 5518–5525.
57 A. Laukkanen, F. M. Winnik and H. Tenhu, *Macromolecules*, 2005, **38**, 2439–2448.
58 S. Binauld, L. Delafresnaye, B. Charleux, F. D'Agosto and M. Lansalot, *Macromolecules*, 2014, **47**, 3461–3472.
59 C. S. Chern, *Prog. Polym. Sci.*, 2006, **5**, 443–486.
60 K. Yan; and Y. Luo, *React. Chem. Eng.*, 2017, **2**, 159–167.
61 J. Qiu, B. Charleux and K. Matyjaszewski, *Prog. Polym. Sci.*, 2001, **26**, 2083–2134.
62 P. B. Zetterlund, *Polym. Chem.*, 2011, **2**, 534–549.
63 L. K. E. A. Abdelmohsen, R. S. M. Rikken, P. C. M. Christianenvan, J. C. M. Hest and D. A. Wilson, *Polymer*, 2016, **107**, 445–449.
64 V. Boyko, A. Pich, Y. Lu, S. Richter, K. Arndt and H. P. Adler, *Polymer*, 2003, **26**, 7821–7827.
65 E. Constable, C. S. Mundwiler, W. Meier and C. Nardin, *Chem. Commun.*, 1999, 1483–1484.
66 W. Schärtl, *Light scattering from polymer solutions and nanoparticle dispersions*, Springer, Berlin, 2007.
67 H. Senff; and W. Richtering, *Colloid Polym. Sci.*, 2000, **278**, 830–840.
68 H. Dou, M. Jiang, H. Peng, D. Chen and Y. Hong, *Angew. Chem., Int. Ed.*, 2003, **42**, 1516–1519.
69 N. J. Warren, O. O. Mykhaylyk, A. J. Ryan, M. Williams, T. Doussineau, P. Dugourd, R. Antoine, G. Portale and S. P. Armes, *J. Am. Chem. Soc.*, 2015, **137**, 1929–1937.